

Tagging nucleon structure functions by heavy particle detection in deep inelastic electron-ion scattering

C. Ciofi degli Atti, L.P. Kaptari¹ and S. Scopetta²

*Department of Physics, University of Perugia and
Istituto Nazionale di Fisica Nucleare, Sezione di Perugia,
Via A. Pascoli, I-06100 Perugia, Italy*

Abstract

It is shown that in deep inelastic electron - ion collisions the detection, in coincidence with the scattered electron, of a nucleus $A - 1$ in the ground state, as well as a nucleon and a nucleus $A - 2$ also in the ground state, may provide unique information on several long standing problems, such as the origin of the EMC effect, the possible medium modifications of the nucleon structure functions, and the nature of Nucleon-Nucleon correlations.

PACS: 13.40.-f, 21.60.-n, 24.85.+p, 25.60.Gc

KEYWORDS: semi-inclusive reactions; nucleon structure functions; medium effects

¹On leave from Bogoliubov Laboratory of Theoretical Physics, JINR, 141980, Dubna, Moscow reg., Russia

²At present at Institut für Kernphysik, Universität Mainz, Joh.-Joachim-Becher-Weg 45, D-55099 Mainz, Germany.

At present the possibilities offered by an electron-ion collider for investigating the properties of nucleons and nuclei are being discussed. In view of the capabilities of such a collider to detect heavy nuclear fragments resulting from the initial collision [1], we would like to suggest a new kind of semi-inclusive process, and illustrate the unique role it could play in clarifying several long standing problems, such the origin of the EMC-effect, the effect of the nuclear medium on the structure of nucleons, and the nature of Nucleon-Nucleon (N-N) correlations. We consider a deep inelastic collision of an electron and a nucleus A and propose to measure, in coincidence with the scattered electron: i) a nucleus $A - 1$ in the ground state; ii) a nucleon and a nucleus $A - 2$ in the ground state. These semi-inclusive processes radically differ from the usual ones considered up to now, namely the detection of a nucleon in coincidence with the electron [2, 3, 4] (only in the case of a deuteron target the usual semi-inclusive process coincides with process “i”). In order to make clear the physics underlying the above processes we remind few basic concepts about nucleon momentum distributions $n(k)(k \equiv |\vec{k}|)$ in the parent nucleus A and the excitation energy of daughter nuclei $A - 1$ and $A - 2$. The probability to have in the parent a nucleon with momentum k and the daughter with the excitation energy E_{A-1}^* , is provided by the nuclear spectral function $P^A(k, E)$, $E = M_{A-1} + M - M_A + E_{A-1}^*$ being the nucleon removal energy, i.e. the energy required to remove a nucleon from a nucleus A leaving $A - 1$ with excitation energy E_{A-1}^* (M is the nucleon mass).

One has (omitting unnecessary here indeces and summations)

$$P^A(k, E) = \sum_{\alpha < F} n_\alpha^A(k) \delta(E - \varepsilon_\alpha) + \sum_{f \neq \alpha} \left| \int d\vec{r} e^{i\vec{k} \cdot \vec{r}} G_{f0}(\vec{r}) \right|^2 \delta[E - (E_{A-1}^f - E_A)], \quad (1)$$

where $E_{A-1}^f = E_{A-1} + E_{A-1}^*$ ($E_{A-1} = M_{A-1} - (A-1)M$), F denotes the Fermi energy, $n_\alpha^A(k)$ is the momentum distribution of a bound shell model state with eigenvalue $\varepsilon_\alpha > 0$, and G_{f0} is the overlap between the wave functions of the ground state of the parent A and the state f of the daughter $A - 1$, the latter having at least one nucleon in the continuum (see for details ref. [5, 6, 7]). The first part of the r.h.s. of Eq. (1) is usually denoted $P_0^A(k, E)$, and the second one $P_1^A(k, E)$. The so called Momentum Sum Rule links the spectral function to

the nucleon momentum distribution, viz.

$$n^A(k) = \int_{E_{\min}}^{\infty} P^A(k, E) dE = \sum_{\alpha < F} n_{\alpha}^A(k) + \sum_{f \neq \alpha} \left| \int d\vec{z} e^{i\vec{k} \cdot \vec{z}} G_{f0}(\vec{z}) \right|^2, \quad (2)$$

where $E_{\min} = E_{A-1} - E_A$. It can therefore be seen that $n_0^A(k) \equiv \sum_{\alpha < F} n_{\alpha}^A(k) = \int_{E_{\min}}^{\infty} P_0^A(k, E) dE$ represents the momentum distribution in the parent, when the daughter is either in the ground state or in hole states of the parent, whereas $n_1^A(k) \equiv n^A(k) - n_0^A(k) = \int_{E_{\min}}^{\infty} P_1^A(k, E) dE$ represents the momentum distribution in the parent, when the daughter is left in highly excited states with at least one particle in the continuum; this means that $n_0^A(k)$ is the momentum distribution of weakly (shell model) bound nucleons, while $n_1^A(k)$ is the one of deeply bound nucleons generated by N-N correlations. A realistic model for the latter leads to the following form of the corresponding spectral function $P_1^A(k, E)$ [5, 6, 7]

$$P_1^A(k, E) = \int d^3 k_{cm} n_{rel}^A \left(|\vec{k} - \vec{k}_{cm}/2| \right) n_{cm}^A(|\vec{k}_{cm}|) \delta \left[E - E_{thr}^{(2)} - \frac{(A-2)}{2M(A-1)} \cdot \left(\vec{k} - \frac{(A-1)\vec{k}_{cm}}{(A-2)} \right)^2 \right], \quad (3)$$

where n_{rel}^A and n_{cm}^A are, respectively, the relative and Center of Mass momentum distributions of a correlated pair. Let us now discuss the two processes we are interested in: the first one is the $A(e, e'(A-1))X$ depicted in Fig. 1 (a), where $A-1$ denotes a nucleus detected with low momentum and in the ground state (or in a hole state of the target, the energy interval of these states being roughly 20 MeV for a medium weight nucleus). The second process, depicted in Fig. 1 (b), is supposed to occur because of N-N correlations and therefore, according to eq. (3), implies the detection of a nucleon with high momentum \vec{p}_2 and a nucleus in the ground or low excited states, with low-momentum $\vec{P}_{A-2} \equiv -\vec{k}_{c.m.} = -(\vec{k} + \vec{p}_2)$ ($\vec{k} \equiv \vec{p}_1$). In what follows, kinematics and differential cross sections will be given in the ion rest frame; boost trasformations to the laboratory system are straightforward. The differential cross section for the first process in Impulse Approximation (IA) has the following form

$$\sigma_1^A \equiv \frac{d\sigma^A}{d\mathcal{E}'_k d\Omega'_k d\vec{P}_{A-1}} = K^A(x_{Bj}, Q^2, y^A) z^A F_2^{N/A}(x_{Bj}/z^A, Q^2) n_0^A(|\vec{P}_{A-1}|), \quad (4)$$

where $\vec{P}_{A-1} \equiv -\vec{p}_1$ and the kinematical factor $K^A(x_{Bj}, Q^2, y^A)$ is

$$K^A(x_{Bj}, Q^2, y^A) = \frac{4\alpha^2}{Q^6} 2M\mathcal{E}_k \mathcal{E}'_k x_{Bj} \cdot \left(\frac{y}{y^A} \right)^2 \left[\frac{(y^A)^2}{2} + (1 - y^A) - \frac{p_1^2 x_{Bj}^2 (y^A)^2}{z_A^2 Q^2} \right], \quad (5)$$

with $x_{Bj} = Q^2/2M\nu$; $y = \nu/\mathcal{E}_k$; $Q^2 = -q^2 = -(k_e - k'_e)^2$, $y^A = (p_1 \cdot q)/(p_1 \cdot k_e)$, $z_A = \frac{p_1 \cdot q}{M\nu} = p_{10} - |\vec{p}_1| \eta \cos \alpha/M$, $\eta = |\vec{q}|/\nu$, $\cos \alpha = \vec{p}_1 \cdot \vec{q}/|\vec{p}_1||\vec{q}|$, $p_1^0 = M_A - \sqrt{(M_{A-1} + E_{A-1}^*)^2 + \vec{P}_{A-1}^2}$, and $n_0^A(|\vec{P}_{A-1}|)$ is the momentum distribution of the hit nucleon removed from the nucleus A leaving the detected $(A-1)$ nucleus in the ground state.

Two issues have to be addressed here: i) the validity of eq. (4), which is based on the IA, and ii) how the process can be used to obtain non-trivial information on the nucleon structure functions. To both ends we are helped by the fact that F_2 and n_0^A are fairly well known for the proton and for low values of $|\vec{P}_{A-1}|$; therefore, starting from a target (Z, N) and detecting a $(Z-1, N)$ ion, the cross section can be related to known proton properties. Moreover, it should also be considered that y^A and z_A depend very weakly upon A , since we are dealing with low momenta and low removal energies ($z_A \sim 1 - |\vec{p}_1| \eta \cos \alpha/M$). As a result, one has $K^A(x_{Bj}, Q^2, y^A) \sim K^N(x_{Bj}, Q^2, y) = (4\alpha^2/Q^6) 2M\mathcal{E}_k \mathcal{E}'_k x_{Bj} (y^2/2 + 1 - y - Q^2/4\mathcal{E}_k^2)$, the relation holding exactly in the Bjorken limit. In order to check the validity of the reaction mechanism let us consider the following quantity:

$$\begin{aligned} R(x_{Bj}, z_A, z_{A'}, \vec{P}_{A-1}, Q^2) &= \frac{\sigma_1^A}{\sigma_1^{A'}} = \frac{K^A}{K^{A'}} \frac{z_A F_2^{N/A}(x_{Bj}/z_A, Q^2)}{z_{A'} F_2^{N/A'}(x_{Bj}/z_{A'}, Q^2)} \frac{n_0^A(|\vec{P}_{A-1}|)}{n_0^{A'}(|\vec{P}_{A-1}|)} \\ &\longrightarrow \frac{z_A F_2^{N/A}(x_{Bj}/z_A, Q^2)}{z_{A'} F_2^{N/A'}(x_{Bj}/z_{A'}, Q^2)} \frac{n_0^A(|\vec{P}_{A-1}|)}{n_0^{A'}(|\vec{P}_{A-1}|)}. \end{aligned} \quad (6)$$

It can be seen that by investigating the above ratio as a function of $|\vec{P}_{A-1}|$ keeping x_{Bj} and α fixed (so that $z_A = z_{A'}$), one gets $R(x_{Bj}, z_A, z_{A'}, |\vec{P}_{A-1}|, Q^2) = n_0^A(|\vec{P}_{A-1}|)/n_0^{A'}(|\vec{P}_{A-1}|)$, and since for low values of $|\vec{P}_{A-1}|$ the momentum distributions are well known, $R(x_{Bj}, z_A, z_{A'}, |\vec{P}_{A-1}|, Q^2)$ can be used to check the validity of the spectator mechanism. Fig. 2 illustrates the expected behaviour of the ratio for $A = 2$, and different values of A' (numerically, we found that $y^A = y$, $K^A = K^N$, $F_2^{N/A}(x_{Bj}/z_A)/F_2^{N/A'}(x_{Bj}/z_{A'}) = 1$ with an accuracy of few per cents). It can be seen from Fig. 2 that the rapid variation of the ratio generated by the variation of $n_0^A(|\vec{P}_{A-1}|)$ can represent a significant check of the spectator mechanism. The experimental

check of the prediction presented in Fig. 2 is a prerequisite for any further measurements, since any deviation from this prediction represents strong indications of some drawbacks of the spectator model.

Let us now consider the possibility to investigate the nucleon structure functions; this has been recently addressed in ref. [4], where the ratio $D(e, e'p)X/D(e, e'n)X$ has been considered in order to investigate the neutron to proton structure function ratio. Here we are interested in emphasizing the origin of the EMC-effect and possible medium modifications of the nucleon structure functions. To this end in Fig. 3 we show the ratio (6) vs. x_{Bj} for $A' = 2$ and various values of A , calculated at fixed value of $|\vec{P}_{A-1}|$ chosen such that $z_D = z_A$. In such a way the nucleon structure functions depend only upon x_{Bj} and the ratio is a constant (curves (a)) with the absolute value given by the ratio of the momentum distributions. On the contrary, if we consider the Q^2 -rescaling model [8] with $Q_A^2 = \xi_A(Q^2)Q^2$, we get an A -dependent ratio having an EMC-like behaviour (curves (b)). Therefore, one may conclude that these processes may serve as a tool to distinguish various interpretations of the EMC-effect. In order to better emphasize the difference between x -rescaling and Q^2 -rescaling models, we have calculated the same ratio at large values of $|\vec{P}_{A-1}|$ and not such that $z_A = z_D$; the latter condition leaves unaffected Q^2 -rescaling but it does affect the x -rescaling since the ratio will now depend upon $x_A = x_{Bj}/z_A$, with $x_D > x_A$, because of the important role of the kinetic energy in the definition of z_D ($z_D \approx (1 - p_1^2/2M^2) < z_A$). This effect is clearly seen in Fig. 4, where the ratio calculated within the x -rescaling model is predicted to increase, whereas the Q^2 -rescaling model gives again the EMC-like behaviour.

In closing we would like to stress that the semi-inclusive processes on weakly bound nucleons that we have analyzed, can be used to investigate the ratio of the neutron to proton structure functions by performing experiments $A(e, e'A - 1)X$ on mirror nuclei or $A(e, e'N - 1)X$ and $A(e, e'Z - 1)X$ on the same isoscalar target.

We address now the important issue of a possible medium modification of the nucleon structure functions. The semi-inclusive process offers the possibility to investigate the nucleon structure function for weakly and deeply bound nucleons separately. To this end one has to consider the process $A(e, e'N_2(A - 2))X$ depicted in Fig. 1 (b).

The differential cross section of such a process in IA reads as follows

$$\sigma_2 \equiv \frac{d\sigma^A}{d\mathcal{E}'_k d\Omega_{k'} d\vec{P}_{A-2} d\vec{p}_2} = K^A(x_{Bj}, Q^2, y^A) \cdot z_A F_2^{N/A}(x_{Bj}/z_A, Q^2) n_{cm}^A(|\vec{P}_{A-2}|) n_{rel.}^A(|\vec{p}_2 + \vec{P}_{A-2}/2|), \quad (7)$$

where the notations are the same as in the previous process. In spite of the fact that eqs. (4) and (7) are very similar, the underlying physics is completely different, since the nucleon structure function $F_2^{N/A}(x_{Bj}/z_A, Q^2)$ in the first case represents the quark distribution in a nucleon which is almost free, while in the second case the hit nucleon is strongly bound in the parent nucleus and its structure function may be affected by the so-called off-mass-shell deformations (see, for instance refs. [9, 10]). As a matter of facts, if the nucleon structure function could be extracted from the cross section (7) and compared with the one obtained from the cross section (4), a direct comparison of nucleon structure functions for weakly and deeply bound nucleons can, for the first time, be carried out.

It should be pointed out that, since kinematically y^A is connected to high momenta $|\vec{p}_2|$, the factor $K^A(x_{Bj}, Q^2, y^A)$ may strongly differ from $K^N(x_{Bj}, Q^2, y)$, unless proper kinematical conditions are chosen, which turn out to be small values of x_{Bj} or the Bjorken limit, $Q^2 \rightarrow \infty$. Nevertheless, we will now show that, in this process, it is still possible to investigate separately the momentum distribution and the structure functions of strongly bound nucleons. First of all we choose a combination of kinematical variables such as to assure that $K^A = K^N$. We found that for $Q^2 = 20$ GeV 2 and $x_{Bj} = 0.05$, the direction of the transferred momentum \vec{q} coincides, in the frame where the target is at rest, with the electron beam direction ($\theta_{\hat{k}q} \approx 2^0$); in this case, $y^A \simeq y$ and $K^A \simeq K^N$ (our numerical estimates show that K^A/K^N varies from 0.99 at $|\vec{p}_2| = 350$ MeV to 0.96 at $|\vec{p}_2| = 1$ GeV); in the laboratory system, adopting realistic figures for a possible collider, i.e. $\mathcal{E}_k \approx 5$ GeV, $T_N =$ (kinetic energy per nucleon) ≈ 25 GeV [1], the chosen values of Q^2 and x_{Bj} correspond to $\mathcal{E}'_k \approx 2$ GeV; $\theta_{\hat{k}k'} \approx 90^0$ (in the ion rest frame they correspond to $\mathcal{E}_k \sim 260$ GeV, $\mathcal{E}'_k \approx 50$ GeV; $\theta_{\hat{k}k'} \approx 2^0$).

The validity of eq. (7) can now be tested in the following way. We will take advantage

of the observation [11] that for high values of $|\vec{p}_1|$ the nucleon momentum distribution for a complex nucleus turns out to be the rescaled momentum distribution of the deuteron with very small A dependence (unlike what happens for the low momentum part of $n(k)$ (cf. Fig. 2)). Let us consider the following ratio:

$$\begin{aligned} R(x_{Bj}, z_A, z_{A'}, Q^2, \vec{P}_{A-2}, \vec{p}_2) &\equiv \frac{\sigma_2^A(x_{Bj}, Q^2, \vec{P}_{A-2}, |\vec{p}_2|)}{\sigma_2^{A'}(x_{Bj}, Q^2, \vec{P}_{A-2}, |\vec{p}_2|)} \\ &= \frac{z_A}{z_{A'}} \frac{F_2^{N/A}(x_{Bj}/z_A, Q^2)}{F_2^{N/A'}(x_{Bj}/z_{A'}, Q^2)} \cdot \frac{n_{rel.}^A(p_{rel.})}{n_{rel.}^{A'}(p_{rel.})}, \end{aligned} \quad (8)$$

where $p_{rel} = |\vec{p}_2 + \vec{P}_{A-2}/2|$. Let us keep fixed $|\vec{P}_{A-2}|$; then, if we could make $F_2^{N/A} \simeq F_2^{N/A'}$, the ratio, measured at $p_{rel} \geq 2-3 \text{ fm}^{-1}$, would be a constant, since $n_{rel.}^A \propto n^D$ for any value of A . The condition $F_2^{N/A} \simeq F_2^{N/A'}$ can be fulfilled by properly choosing \vec{p}_2 and \vec{P}_{A-2} for, if Eq. (3) is correct, the off-shell energy of the hit nucleon is $p_1^0 = M_A - \sqrt{(M_{A-1} + E_{A-1}^*)^2 + \vec{p}_1^2}$, with $E_{A-1}^* \simeq \frac{(A-2)}{2M(A-1)} |\vec{p}_1|^2$, so that $z_A \simeq 1 - \frac{E_{min}^A}{2M} - \frac{(A-2)|\vec{p}_1|^2}{2M^2(A-1)} - \frac{|\vec{p}_1|}{M} \cos \alpha$, and by properly choosing \vec{p}_2 and \vec{P}_{A-2} ($\vec{p}_1 = -(\vec{p}_2 + \vec{P}_{A-2})$) one can make $z_A \simeq z_{A'}$, i.e. $F_2^{N/A} \simeq F_2^{N/A'}$ (note that for large values of $|\vec{p}_1|$, as it is in our case, and large values of A , the dependence of z_A upon A is unessential). Another possibility would be to consider in Eq. (6) $A = A' = 2$, with the denominator taken at some fixed and high value of $|\vec{P}_{A-1}| = |\vec{p}_1| = \tilde{p}$, so that $\tilde{z}_{D'} \simeq 1 - \frac{E_D}{M} - \frac{\tilde{p}^2}{2M^2} - \frac{\tilde{p}}{M} \cos \alpha$. If we now consider Eq. (8) with $A = A' > 2$ and the denominator taken at the value $|\vec{p}_1| = |\vec{p}_2 + \vec{P}_{A-1}| = \tilde{p}$, so that $\tilde{z}_{A'} \simeq 1 - \frac{E_{min}^A}{M} - \frac{(A-2)\tilde{p}^2}{2M^2(A-1)} - \frac{\tilde{p}}{M} \cos \alpha$, the ratio (8) plotted versus p_{rel} for a fixed value of \vec{P}_{A-2} should behave as the ratio (6).

If such a deuteron – like behaviour of Eq. (8) is found, this would represent a stringent test of the spectator model, and off-mass-shell effects can be investigated by comparing the structure functions measured in the $A - 1$ and $A - 2$ processes. To this end:

- i) in the case of (A-1) one may fix $|\vec{P}_{A-1}| = 50 \text{ MeV}$ (weakly bound nucleon), $Q^2 = 20 \text{ GeV}^2$ and vary x_{Bj} from 0 to 0.5 and the angle of \vec{P}_{A-1} from 0° to 180° . One finds that $K^A = K^N$ within $\pm 3\%$. This condition allows one to vary the argument of the nucleon structure function from 0 to 0.6 and to study F_2^N in this interval. Note that in order to exclude the influence of the momentum distribution, one may vary any variables but $|\vec{P}_{A-1}|$;
- ii) in the case of (A-2), one can choose $|\vec{P}_{A-2}| = 50 \text{ MeV}$, $|\vec{p}_2| = 700 \text{ MeV}$ (deeply bound nucleon), the angle between them constant, e.g. 180° , $Q^2 = 20 \text{ GeV}^2$ and $x_{Bj} = 0.05$.

Then varying the angle between \vec{p}_2 and \vec{q} from zero to the kinematical limit $x_{Bj}/z = 1$, one may obtain the structure function of a strongly bound nucleon in the whole interval of x . A detailed treatment of the $A(e, e'N_2(A-2))X$ process with partial account of Final State Interactions due to both the $N_2 - (A-2)$ rescattering and fragmentation of the hit nucleon will be presented elsewhere.

Acknowledgements

One of us (C.C.d.A.) would like to thank V. Metag, D. v Harrach and A. Schäfer for useful discussions during the Working Groups on “Long Term Perspectives of GSI”.

References

- [1] V. Metag, D. v Harrach and A. Schäfer, private communication.
- [2] L.L. Frankfurt and M.I. Strikman, Phys. Rep. 160 (1988) 235.
- [3] C. Ciofi degli Atti and S. Simula, Phys. Lett. B 319 (1994) 23.
- [4] S. Simula, e-print archives nucl-th/9605024, to be published in Phys. Lett. B; W. Melnitchouk, M. Sargsian, M.I. Strikman, e-print archives nucl-th/9609048.
- [5] C. Ciofi degli Atti, S. Simula, L.L. Frankfurt and M.I. Strikman, Phys. Rev. C 44 (1991) R7.
- [6] M. Baldo, M. Borromeo and C. Ciofi degli Atti, Nucl. Phys. A 604 (1996) 429.
- [7] C. Ciofi degli Atti and S. Simula, Phys. Rev. C 53 (1996) 1689.
- [8] F.E. Close, R.G. Roberts and G.G. Ross, Nucl. Phys. B 296 (1988) 582.
- [9] W. Melnitchouk, A.W. Schreiber and A.W. Thomas, Phys. Rev. D 49 (1994) 1199; S.A. Kulagin, G. Piller and W. Weise, Phys. Rev. D 50 (1994) 1154.
- [10] A.Yu. Umnikov, L.P. Kaptari and F. Khanna, Phys. Rev. C 53 (1996) 377.

[11] J.G. Zabolitzky and W. Ey, Phys. Lett. B 76 (1978) 527; R. Schiavilla, V.R. Pandharipande and R.B. Wiringa, Nucl. Phys. A 449 (1986) 219.

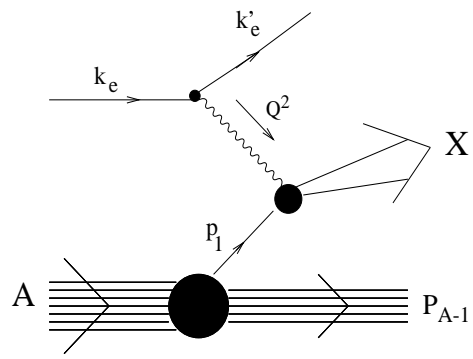
Captions

Figure 1: Kinematics for the semi-inclusive processes in the impulse approximation.

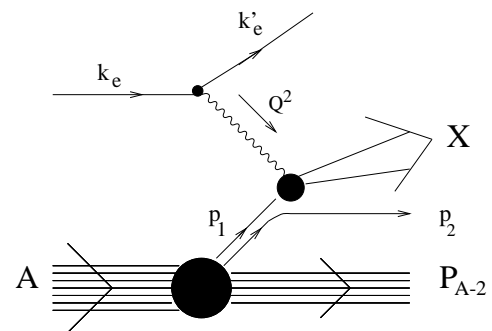
Figure 2: The ratio $R(x_{Bj}, z_D, z_A, |\vec{P}_{A-1}|, Q^2) \equiv \frac{\sigma_1(D)}{\sigma_1(A)} = \frac{z_D}{z_A} \frac{n_D(|\vec{P}_{A-1}|)}{n_A(|\vec{P}_{A-1}|)} \frac{F_2^{N/D}(x_{Bj}/z_D, Q^2)}{F_2^{N/A}(x_{Bj}/z_A, Q^2)}$, (Eq. (6)) calculated for different values of A at fixed x_{Bj} and $\alpha = 90^\circ$; because of the latter condition, z_D differs from z_A at low values of $|\vec{P}_{A-1}|$ by only few percents, so that the behaviour of the curves is given by the ratio $n_D(|\vec{P}_{A-1}|)/n_A(|\vec{P}_{A-1}|)$. The nucleon momentum distributions have been taken from ref. [7].

Figure 3: The ratio $R(x_{Bj}, z_A, z_{A'}, |\vec{P}_{A-1}|, Q^2) \equiv \frac{\sigma_1(A)}{\sigma_1(D)} = \frac{z_A}{z_D} \frac{n_A(|\vec{P}_{A-1}|)}{n_D(|\vec{P}_{A-1}|)} \frac{F_2^{N/A}(x_{Bj}/z_A, Q^2)}{F_2^{N/D}(x_{Bj}/z_D, Q^2)}$, for different values of A at $\alpha = 90^\circ$. For each nucleus $|\vec{P}_{A-1}|$ is chosen such that $z_D = z_A$. Curves labeled (a) correspond to x - rescaling while those labeled (b) correspond to Q^2 -rescaling [8]. The behaviour of the curves is given by the ratio $F_2^{N/A}(x_{Bj}, Q^2)/F_2^{N/D}(x_{Bj}, Q^2)$.

Figure 4: The same ratio as in Fig. 3 but $|\vec{P}_{A-1}|$ is the same for each target, so that the behaviour is governed by the ratio $F_2^{N/A}(x_{Bj}/z_A, Q^2)/F_2^{N/D}(x_{Bj}/z_D, Q^2)$. Since the hit nucleon is an almost free one, $z_A \sim 1 - \frac{E_{min}^A}{M} \sim 1$, whereas $z_D \simeq 1 - \frac{E_D}{M} - \frac{p^2}{2M^2} < 1$, therefore in x - rescaling the ratio is predicted to increase as x_{Bj} increases (curves (a)), whereas in Q^2 rescaling model [8] this ratio has a decreasing behaviour (curves labeled (b)).



a)



b)

C. Ciofi degli Atti, Phys. Lett. B

FIGURE 1

C. Ciofi degli Atti, Phys. Lett. B

FIGURE 2

C. Ciofi degli Atti, Phys. Lett. B

FIGURE 3

C. Ciofi degli Atti, Phys. Lett. B

FIGURE 4

